

Architecture of superstructure on binary blends of core-shell polymer microsphere/diblock copolymers

Koji Ishizu

Department of Polymer Science, Tokyo Institute of Technology 2-12, Ookayama,
 Meguro-ku, Tokyo 152, Japan

(Received 22 August 1996)

The three-phase separated morphologies on binary blends of core-shell polymer microsphere/diblock copolymers (lamellar and spherical morphologies in thermal equilibrium) were studied in two-dimensional aspects using transmission electron microscopy. Ordering rule on these binary blends depended strongly on the blend ratio and the molecular weight of diblock copolymers. New three-phase separated structure in which diblock copolymers were arranged as a honeycomb-like bilayer around the ordered microspheres, appeared by these blendings. © 1997 Elsevier Science Ltd.

(Keywords: superstructure; diblock copolymer; core-shell polymer microsphere)

INTRODUCTION

We reported a variety of the preparations of core-shell polymer microspheres by means of immobilizing microphase-separated spherical domains formed by diblock copolymer films^{1–7}. Such microspheres were stabilized even in a good solvent by highly branched arms. Moreover, it was found from the small-angle X-ray scattering (SAXS) that microspheres were packed in the superlattice of a body-centred cubic (b.c.c.) structure near the overlap concentration (C^*)⁸. This packing structure transformed to the superlattice of a face-centred cubic (f.c.c.) structure in the bulk film^{8,9}.

Hierarchical structure transformation of such microspheres could be explained by thermal blob model proposed by Daoud and Cotton¹⁰ as shown in *Figure 1*. The picture presented for a star polymer consists of three regions, a central core (region I), a shell with semidilute segment density in which the arms have their unperturbed chain conformations (region II), and an outer shell in which the arms of the star assume a self-avoiding conformation (region III). In a core-shell microsphere, the crosslinked core domain can be regarded as the central core of region I. The arms in the shell part can be seen as a succession of growing blobs in regions II and III. A b.c.c. ordering of these microspheres appeared close to the C^* . The crosslinked cores did not interpenetrate with each other and the core-shell microspheres were compatible with shell parts during solvent evaporation. As a result, a packing structure such as an f.c.c. lattice appeared in the bulk film. This is the most efficient way of packing spheres.

Thus, the core-shell microspheres can be considered as the smallest unit in the microphase-separated structure. The properties of the microspheres in the solvent area governed not by the core but the shell chains. So, the core-shell microspheres can be regarded as the spherical macromolecule with multi-arms in the solvent. These microspheres can be used as composite materials in

blends for the introduction of spherical microdomains into a matrix.

In general, the microphase separation with three phases can be obtained for an ABC triblock copolymer. The morphology of ABC triblock copolymers has been suggested by Riess *et al.*¹¹. More recently, interesting morphologies of microphase separation with three phases have been reported for ABC triblock copolymers^{12–15}. On the other hand, we reported microphase separation with three phases in the blend system of AB/AC diblock copolymer micelles¹⁶. In this blend, two spherical B and C microdomains were dispersed at random in an A matrix. Moreover, we have investigated the morphologies of binary blends of well-ordered core-shell microsphere/AB diblock copolymers, which form lamellar or spherical microdomains in thermal equilibrium morphology^{17,18}. As a result, three-phase separated morphologies such as honeycomb-like structure and two spherical domains dispersed in a matrix.

In this article, we studied the architecture of superstructure on binary blends of core-shell microsphere/AB diblock copolymers (lamellar and spherical morphologies in thermal equilibrium) binary blends. The poly(4-vinylpyridine) (P4VP) core-polystyrene (PS) shell microsphere synthesized previously was used. Poly[styrene(S)-b-isoprene(I)] diblock copolymers [lamella and polyisoprene (PI) sphere], synthesized by anionic polymerization, were chosen as the AB diblock copolymers. The morphology of binary blends was investigated by transmission electron microscopy (TEM) as parameters of blend ratio and molecular weight of diblock copolymers.

EXPERIMENTAL

Polymer synthesis and characterization

The well-defined poly(S-b-4VP) and poly(S-b-I)s were

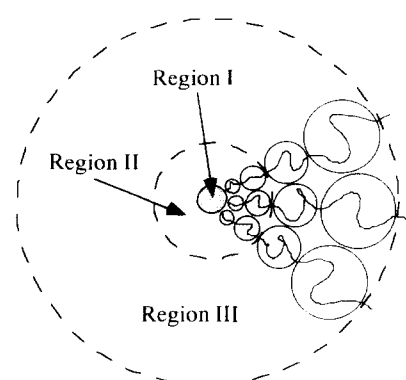


Figure 1 Thermal blob model for star polymer

prepared by the usual sequential anionic polymerization using *n*-butyl lithium (*n*-BuLi) as an initiator in tetrahydrofuran (THF) and in benzene, respectively. Details concerning the synthesis and characterization of these copolymers have been given elsewhere^{1,16}. Table 1 lists the characteristics of the 'monodisperse' diblock copolymers and the microdomain spacings. Where poly(S-b-4VP): SV and poly(S-b-I): SI specimens were cast from 1,1,2-trichloroethane (TCE) and benzene, respectively.

The microdomain structure in SV1 specimen showed the texture of discrete P4VP spheres in a PS matrix. On the other hand, the microdomain structures in SI50 and SI22 specimens showed the texture of PI spheres in a PS matrix and that of PS/PI alternating lamellae, respectively.

Synthesis and characterization of core-shell microsphere

The segregated P4VP chains in a sphere were crosslinked by using quaternization with 1,4-dibromobutane (DBB) vapour at room temperature in the solid state under high vacuum. It was found from i.r. spectra that block copolymer films with P4VP spheres were almost quantitatively quaternized with DBB at the reaction time of 2 days¹. The crosslink density was determined to be 48 mol% by Volhard's titration. Figure 2 shows a TEM micrograph of crosslinked polymer microsphere of SV1 (SV1M) cast from 0.1 wt% TCE/nitrobenzene: 10/1 (v/v) solution. This specimen was stained with osmium tetroxide (OsO₄) vapour. The dark, grey, and white portions indicate the crosslinked P4VP core, shell of PS chains, and carbon support, respectively. In the preparation conditions of this cast specimen, multimolecular micelles were frozen with a structure like the core-shell type microspheres. These microsphere particles had only

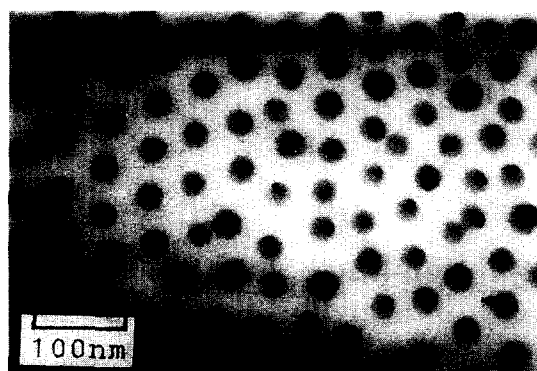


Figure 2 TEM micrograph of crosslinked polymer microsphere of SV1 (SV1M)

Table 2 Characteristics of core-shell polymer microsphere SV1M

Specimen code	$10^{-7} \cdot M_w$	f^a	CD ^b	Domain size (nm) ^c		R_h^d (nm)	C^{**} (wt%)
				P4VP core	External		
SV1M	6.16	550	48	17	24	80	4.8

^a Aggregation number (arm number)

^b Crosslink density of P4VP core

^c Radius estimated by TEM micrographs

^d Hydrodynamic radius of microsphere determined by DLS

^e Calculated by equation: $C^{**} = 3M_w / (4\pi R_h^3 N_A)$, where N_A is Avogadro's number

a narrow particle size distribution. Characteristics of core-shell type microsphere SV1M are listed in Table 2.

Binary blends of microsphere with diblock copolymers

The binary blends of the diblock copolymers with the P4VP core-PS shell microsphere were prepared from the TCE/nitrobenzene: 10/1 (v/v) mixed solution at 1.0 wt% polymer concentration.

Morphology observations

Ultrathin specimens of the block copolymers were prepared for TEM by allowing a drop of a TCE (SV) or benzene (SI), respectively, on a copper grid coated with a carbon substrate to evaporate very slowly at room temperature. For observation of the packing state of binary blends in the bulk, ultrathin films (80 nm thickness) were prepared by cutting the films with a microtome (Reinhert-Nissei Ultracut N). The specimens were stained with OsO₄ over 24 h at room temperature.

Table 1 Characteristics of diblock copolymers and domain spacings

Specimen ^a code	Block copolymer		Shape	Domain size ^d (nm)			
	$10^{-4} \cdot M_n^b$	P4VP (PI) ^c block (wt%)		\bar{R}_{P4VP}	R_{PI}	D_{PS}	\bar{D}_{PI}
SV1	11.2	24	P4VP spheres	17			
SI22	7.0	50	PI/PS lamellae			4.5	4.5
SI50	3.2	18	PI spheres		8		

^a SV, poly(S-b-4VP); SI, poly(S-b-I) diblock copolymer

^b Measured by osmometry or vapour pressure osmometer

^c Determined by ¹H n.m.r. in CDCl₃

^d Determined by means of electron microscopy for specimens from TCE (SV1) or benzene (SI22 and SI50). \bar{R}_{P4VP} (R_{PI}) = average radius of P4VP (PI) spherical domains; \bar{D}_{PS} (\bar{D}_{PI}) = average distance of PS (PI) lamellar domains

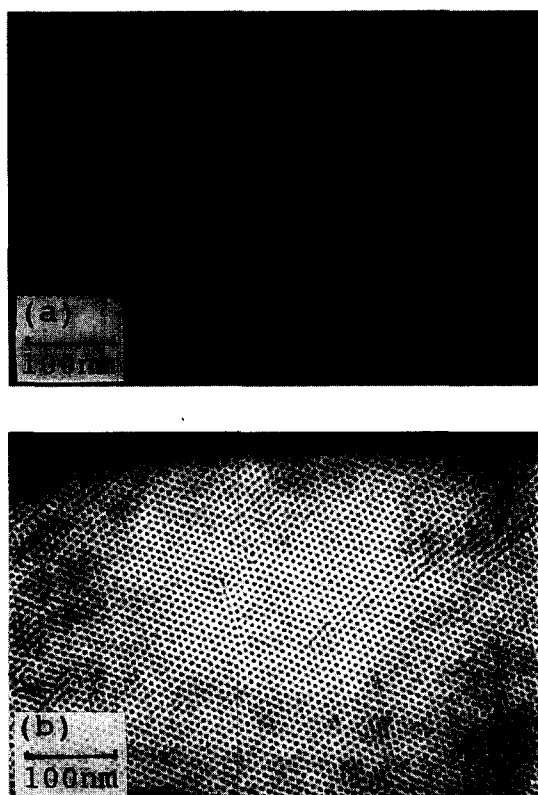


Figure 3 TEM micrographs of SI diblock copolymers: (a) SI22; (b) SI50

The morphology observations were performed with a Hitachi H-500 TEM at 75 kV.

RESULTS AND DISCUSSION

Figure 3 shows typical TEM micrographs of SI diblock copolymers cast from benzene. The dark portions correspond to the PI phases selectively stained with OsO_4 . The thermal equilibrium morphology of SI22 (50 wt% PI) is a structure of alternating PI/PS lamellar microdomains. On the other hand, the microdomain structure in the SI50 specimen (82 wt% PI) shows the texture of discrete PI spheres in a PS matrix. The characteristics of the SI diblock copolymers and the microdomain spacings are collected in Table 1.

It was mentioned in the Introduction that the core-shell microspheres were packed in the superlattice of an b.c.c. structure near the C^* . To form the superlattice with microsphere on drying the blend solution, the polymer concentration of the blending solution was maintained at 1.0 wt%, i.e. below the C^* (4.8 wt%). Figure 4a shows the TEM micrograph of binary blend film of SV1M microsphere with SI50 diblock copolymer (in two dimensions; weight fraction of diblock copolymer in binary blend,

$$\frac{[\text{diblock copolymer}]}{[\text{diblock copolymer}] + [\text{SV1M}]} \gamma = 0.5 (\text{wt/wt}).$$

The dark portions in the micrograph correspond to P4VP and PI phases stained with OsO_4 . It is found from this texture that six small spherical microdomains are arranged around each large spherical microdomain. The large spherical microdomains seem to be hexagonally packed in two dimensions. The diameters of spherical microdomains were approximately 15 and 35 nm. These diameters agreed well with those of the PI spheres and

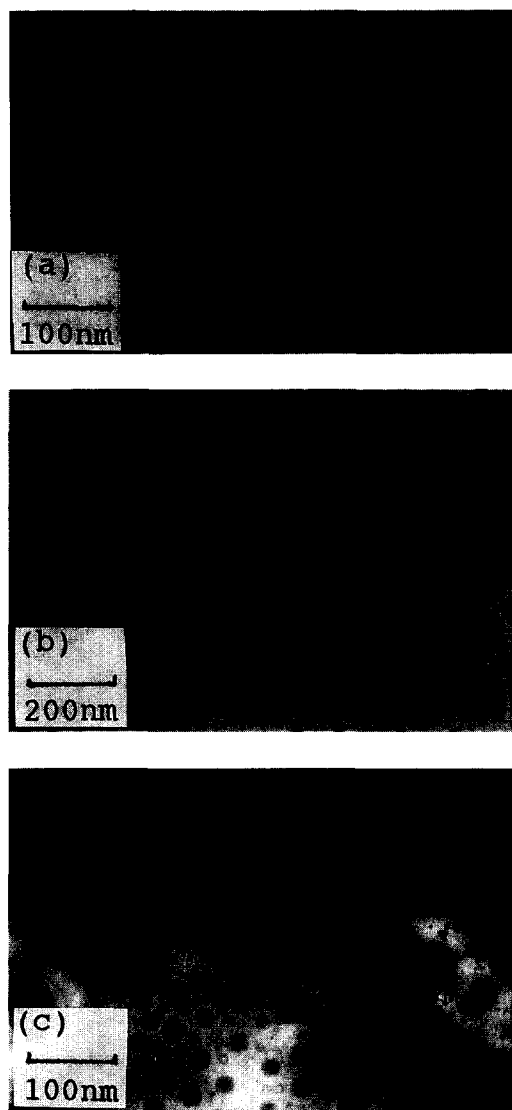


Figure 4 TEM micrographs of binary blend films: (a) SV1M/SI50, $\gamma = 0.5$; (b) SV1M/SI22, $\gamma = 0.5$; (c) SV1M/SI22, $\gamma = 0.6$

P4VP cores, respectively. It was therefore concluded that the small spherical microdomain was PI and the large one was the P4VP core.

Subsequently, we investigated the packing patterns of two spherical domains using the radial distribution function $g_{nm}(r)$ from sphere n to sphere m . Figure 5 shows the radial distribution functions of binary blend of SV1M with SI50 in two dimensions. For the radial distribution function, 1 and 2 indicate the P4VP core and the P2VP spherical microdomain, respectively. From TEM observation (Figure 4a), the arrangement of two kinds of spheres was assumed as follows: the P4VP cores are packed hexagonally on top of the hexagons surrounding the P4VP cores. Figure 6 shows the schematic arrangement of the spheres in this binary blend.

First, the radial distribution function between P4VP cores in the blend, $g_{11}(r)$ was estimated. Three peaks are observed for the $g_{11}(r)$ as shown in Figure 5a. When the P4VP cores are packed in such schematic arrangement, the peaks of $g_{11}(r)$ should appear at $r = a$, $\sqrt{3}a$ and $2a$ for the first, second and third generations, respectively. Three peaks were observed at $a = 59.5$, 102.8 and 119.2 nm, and the ratio of the distances was 1/1.73/2.00.

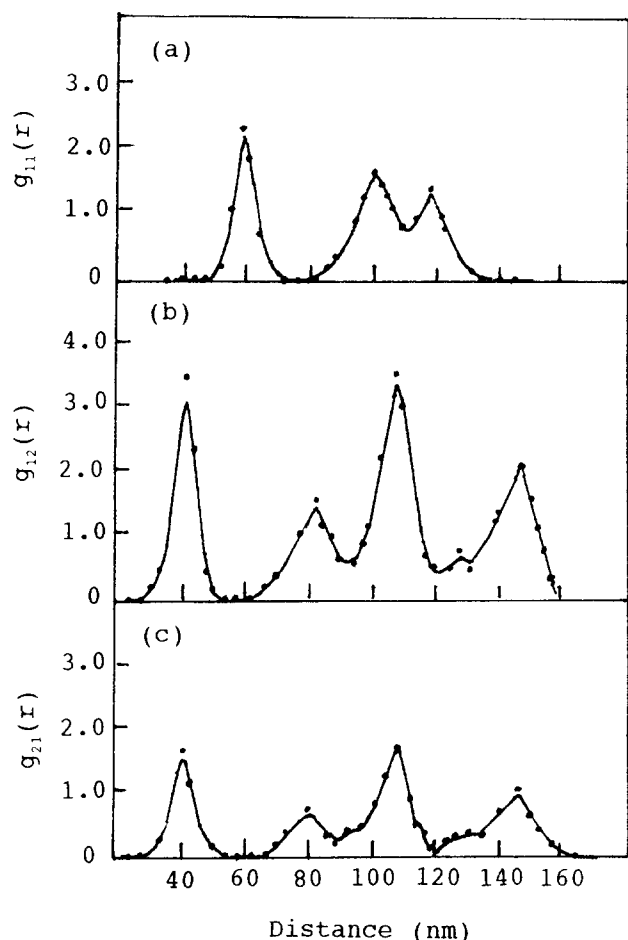


Figure 5 Radial distribution functions: (a) between P4VP cores of microspheres; (b) from P4VP core to PI sphere; (c) from PI sphere to P4VP core

These values were well in agreement with those calculated from the schematic arrangement.

Two radial distribution functions, $g_{12}(r)$ and $g_{21}(r)$ were obtained between the P4VP core and PI sphere (Figures 5b and c). In general, both peaks of $g_{12}(r)$ and $g_{21}(r)$ should appear at the same r values. For the schematic packing, the peaks appeared at $r = b, 2b, \sqrt{7}b$ and $\sqrt{13}b$, for the first, second, third and fourth generations, respectively (see Figure 6). For both $g_{12}(r)$

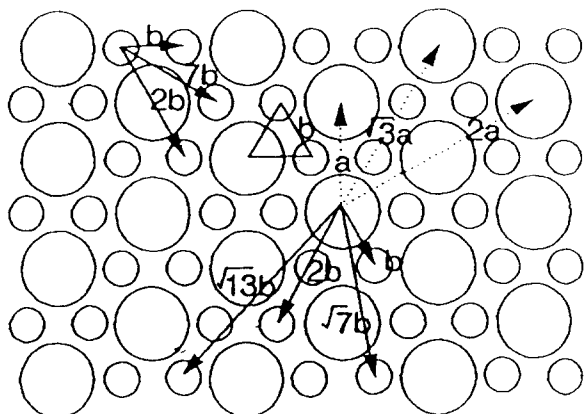


Figure 6 Schematic arrangement of microdomains of microsphere and diblock copolymer

and $g_{21}(r)$, the peaks were observed at $b = 40.8, 81.3, 108.2$ and 146.8 nm. The ratio of the distances was $1/1.99/2.65/3.60$. These values were also in good agreement with those calculated from the schematic arrangement. Moreover, the peak heights of $g_{12}(r)$ were twice as large as those of $g_{21}(r)$. This result also supports the schematic arrangement of the spheres shown in Figure 6.

Next, we investigated the possibility of superlattice formation on binary blends of SV1M microsphere with SI22 diblock copolymer (lamellar morphology), varying the blend fraction γ . Figure 4b shows the TEM micrograph of binary blend film with $\gamma = 0.5$ (in two dimensions). The morphology obtained shows the texture that all of the spherical microdomains are surrounded by a grey thin layer similar to a cell wall. The domain sizes of such spheres and thin layers were agreement with those of P4VP cores of SV1M and PI lamellar domains of SI22, respectively. It was therefore concluded that P4VP cores were arranged in a honeycomb-like PI layer. Moreover, these P4VP cores were packed hexagonally. On the other hand, Figure 4c shows the TEM micrograph of binary blend film with $\gamma = 0.6$. It is found from this texture that the P4VP cores are locally ordered in a honeycomb-like morphology, but wide white regions exist in some portions of the TEM micrograph. These regions may correspond to PI/PS alternating lamellar microdomains of the SI22 diblock copolymer. In this blend fraction, the SI22 was macroscopically phase separated and diblock copolymer formed the lamellar structure individually.

From the above results, the segment arrangement in this three phase-separated morphology with a honeycomb-like structure can be represented schematically as shown in Figure 7. The cell of the microspheres has an hexagonal surface, and the SI diblock copolymer forms a bilayer between the microspheres. The hexagon is surrounded with a PI bilayer indicating that the unit cell of the microsphere is hexagonal in two dimensions. The PS block segments of SI22 are probably miscible with PS arms (common component) in the microsphere shell parts. The appearance of this unique morphology depended strongly not only on the blend fraction but

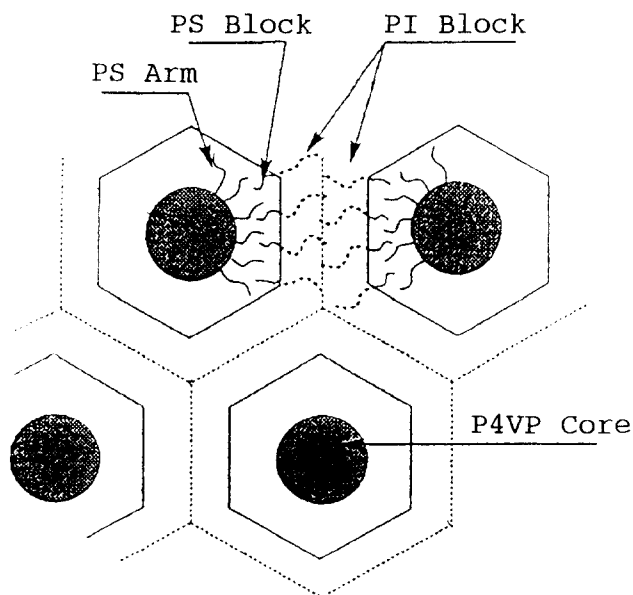


Figure 7 Schematic representation of honeycomb-like structure

also on the molecular weight of SI diblock copolymers. Honeycomb-like morphology has never been observed in the binary blend specimens of SV1M (PS arm, $\bar{M}_n = 8.5 \times 10^4$) with other SI diblock copolymers (lamellar morphology; more than $\bar{M}_n = 3.0 \times 10^4$).

It was found from our works that the core-shell microspheres with multi-arms behaved like hard sphere¹⁹. Hierarchical structure transformation of the core-shell microspheres originates in such topological structure. Semenov²⁰ has treated theoretically the superlattice formation on micelles formed by block copolymer (AB)-homopolymer (A) mixtures. According to his results, the block copolymers form essentially spherical micelles (core-corona type) for minor B-blocks (B-blocks shorter than A-blocks). In the case that homopolymer chains are much shorter than copolymers, shorter homopolymer chains should be able to penetrate into the corona of a micelle; short enough homopolymers will behave as a solvent. In the case of long homopolymer chains, micelles attract each other and therefore they should readily separate and form a copolymer-rich superstructure. At equilibrium, copolymer domains should prefer to retain their symmetric spherical shape, thus leaving gaps filled by homopolymer chains. The energy of the copolymer-homopolymer interfaces is much lower than the energy of the additional elongation of the copolymer chains that should be produced to fill the gaps by the copolymer.

In binary blends of SV1M microsphere with SI22 diblock copolymer, the microspheres behave like hard sphere and form a closed-packed spherical superstructure during solvent evaporation. At equilibrium, the leaving gaps are filled by diblock copolymer chains. Shorter PS block chains may be able to penetrate into the PS arms of microsphere shell parts. However, PI block chains cannot be penetrated into the shell parts due to the repulsion between incompatible block chains. As a

result, PI block chains form a bilayer such as honeycomb-like morphology. Multi-armed star polymer is also expected to behave like a hard sphere. Further study is necessary whether binary blends of multi-armed star polymer with diblock copolymer form or not such honeycomb-like morphology. The results obtained for their phase separation behaviours will be reported in the near future.

REFERENCES

1. Ishizu, K. and Fukutomi, T., *J. Polym. Sci., Polym. Lett. Ed.*, 1988, **26**, 281.
2. Ishizu, K., *Polymer*, 1989, **30**, 793.
3. Ishizu, K. and Önen, A., *J. Polym. Sci., Polym. Chem. Ed.*, 1989, **27**, 3721.
4. Saito, R., Kotsubo, H. and Ishizu, K., *Eur. Polym. J.*, 1991, **27**, 1153.
5. Saito, R., Kotsubo, H. and Ishizu, K., *Polymer*, 1992, **33**, 1073.
6. Ishizu, K., Naruse, F. and Saito, R., *Polymer*, 1993, **34**, 3929.
7. Saito, R., Kawachi, N. and Ishizu, K., *Polymer*, 1994, **35**, 867.
8. Ishizu, K., Sugita, M., Kotsubo, H. and Saito, R., *J. Colloid Interface Sci.*, 1995, **169**, 456.
9. Saito, R., Kotsubo, H. and Ishizu, K., *Polymer*, 1994, **35**, 1747.
10. Daoud, M. and Cotton, J. P., *J. Phys. (Les Ulis, Fr.)*, 1982, **43**, 531.
11. Riess, G., Schlienger, M. and Marti, G., *J. Macromol. Sci.-Phys.*, 1980, **B17**, 355.
12. Mogi, Y., Kotsuji, H., Kaneko, Y., Mori, K., Matsushita, Y. and Noda, I., *Macromolecules*, 1992, **25**, 5408.
13. Auschra, C. and Stadler, R., *Macromolecules*, 1993, **26**, 217.
14. Gido, S. P., Schward, D. W., Thomas, E. L. and Goncalves, M.C. *Macromolecules*, 1993, **26**, 2636.
15. Stadler, R., Auschra, C., Beckmann, J., Krappe, U., Voigt-Martin, I. and Leibler, L., *Macromolecules*, 1995, **28**, 3080.
16. Ishizu, K., Omote, A. and Fukutomi, T., *Polymer*, 1990, **31**, 2135.
17. Saito, R., Kotsubo, H. and Ishizu, K., *Polymer*, 1994, **25**, 1580.
18. Saito, R., Kotsubo, H. and Ishizu, K., *Polymer*, 1994, **35**, 2296.
19. We determined the radius of gyration (R_g) and hydrodynamic radius (R_h) by SLS and DLS, respectively. As a result, the values of R_g/R_h was to be 0.776 (hard sphere; $R_g/R_h = 0.775$).
20. Semenov, A. N., *Macromolecules*, 1993, **26**, 2273.